Indian Journal of Chemistry
Vol. 64, March 2025, pp. 299-305
DOI: 10.56042/ijc.v64i3.8983

Comprehensive DFT analysis on monosodium urate: Implications for gout pathophysiology

M Bouha*[a], M Echajia[a], H Essassaoui[a], Y Aassem[a] & M Berkani[b]

[a] Laboratory of Engineering in Chemistry and Physics of Matter, Department of Chemistry and Environment, Faculty of Science and Technics, Sultan Moulay Slimane University, Beni Mellal, Morocco

[b] Laboratory of Food Engineering and Technologies (LITA), Department of Chemistry and Environment, Faculty of Science and Technics, Sultan Moulay Slimane University, Beni Mellal, Morocco

E-mail: mohamedbouha2@gmail.com

Received 22 February 2024; accepted (revised) 27 February 2025

This research employs advanced Density Functional Theory (DFT) techniques to conduct a comprehensive analysis of monosodium urate ($NaC_5H_3N_4O_3$), a pivotal molecule in gout pathophysiology. The B3LYP/6-311G** method is utilized to explore conformational stability, molecular structure, UV-Vis and IR spectra, as well as electronic properties of monosodium urate. The study reveals intricate information about electronic transitions, molecular vibrations, and orbital interactions, providing a profound understanding of molecular dynamics associated with monosodium urate. Additionally, Nuclear Magnetic Resonance (NMR) analysis predicts precise ^{1}H and ^{13}C chemical shifts, offering nuanced structural insights. Quantum calculations contribute to a thorough characterization of monosodium urate, enhancing our understanding of its molecular intricacies. The findings from this study significantly enhance our comprehension of the underlying molecular mechanisms of gout, shedding light on potential therapeutic interventions. The detailed insights into electronic properties and structural dynamics open new perspectives for the application of monosodium urate in environments influenced by electrical factors. In essence, this research not only expands our knowledge of gout pathophysiology but also presents innovative opportunities for targeted research and therapeutic development.

Keywords: DFT, Chemical descriptor, Monosodium urate, Quantum chemical calculation, Vibrational spectra

Advancements in theoretical and computational chemistry have revolutionized our understanding of complex organic molecules, enabling a thorough characterization of their structural and functional properties[1-3]. In this context, monosodium urate ($NaC_5H_3N_4O_3$) (Fig. 1), a key compound involved in the pathology of gout, has garnered increasing interest for its molecular characterization[4-8]. This crystalline molecule plays a central role in the mechanisms of gout, an inflammatory disease affecting numerous individuals worldwide[9,10]. Understanding the properties of monosodium urate is fundamental to elucidating the biochemical mechanisms of gout and exploring new therapeutic avenues[11-13]. Density Functional Theory (DFT) is a powerful tool for studying molecular properties, offering crucial insights into electronic structure, vibrations, and intermolecular interactions. Our research aims to comprehensively characterize monosodium urate using these methods to determine the physicochemical factors governing crystal formation and growth in gout. Building on previous work, this study focuses on gaining deeper insights into the critical interactions between monosodium urate and biomolecules present in the joints. We will present our methodology, DFT analysis results, and their implications for medical research. This innovative approach holds promise for making significant contributions to scientific knowledge and paving the way for potential new therapeutic strategies for gout.

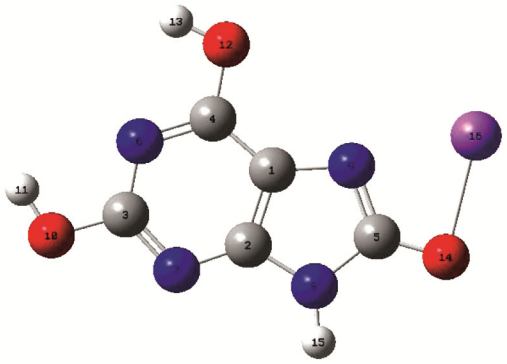

Fig. 1 — Optimized geometric structure with atoms numbering of monosodium urate.

Calculation methods

All calculations were performed using the Gaussian 09 software. The Density Functional Theory (DFT) method was employed, utilizing the B3LYP functional, which combines the non-local exchange function with three Becke parameters and the Lee–Yang–Parr correlation function[14-16]. Calculations were carried out using the 6-311 G (d,p) Pople basis set[17]. Geometric optimizations of molecular structures were conducted in the gas phase, and energy minima were confirmed through frequency calculations. The latter were compared with experimental structural data, demonstrating satisfactory agreement, allowing for a reliable comparison of energies and other physicochemical properties.

Simulated UV–Vis absorption spectra of the monosodium urate molecule were obtained using the DFT method (B3LYP), following an approach established by other researchers[14,18]. The energies of the corresponding Highest Occupied Molecular Orbital (HOMO) and Lowest Unoccupied Molecular Orbital (LUMO) were then used to estimate various parameters of global chemical reactivity, such as chemical potential (μ), electronegativity (χ), electrophilicity index (ω), as well as chemical hardness (η) and softness (S)[19,20].

Furthermore, partial charges were calculated using the Atomic Polarizability Tensor (APT), and the Molecular Electrostatic Potential (MEP) map was generated for the monosodium urate molecule. The molecular dipole moment was also determined in a similar manner. Natural Bond Orbital (NBO) analysis was conducted for certain optimized molecular structures, providing additional insights into charge distribution and the nonlinear optical properties of the molecule.

Results and Discussion

UV-Vis spectral analysis and infrared vibration spectra of the monosodium urate molecule

The UV–Vis spectra, electronic transitions, vertical excitation energies, and oscillator strength were calculated systematically using the Density Functional Theory (DFT) method, considering solvent effects[21-23]. Fig. 2 depicts the UV-Vis spectrum of monosodium urate. DFT analysis suggests a link between its electronic properties and potential involvement in gout. This link is supported by light absorption in the 250-350 nm range, indicating electronic modifications that could influence molecular interactions and solubility. These changes might impact urate crystallization in joints, a key factor in gout development. Further research is needed to understand how electronic properties affect dynamics and biological processes, potentially leading to new insights and avenues for understanding and treating gout.

FT-IR is a method founded on the vibrations of the atoms of a molecule[24,25]. The infrared (IR) spectrum of the monosodium urate neurotransmitter has been registered in the range of fingerprints (0–4000 cm^{-1}). Spectroscopic studies are supplemented by quantum chemical calculations at the level of B3LYP theory by the basis set 6-311G (d, p)[26].

The analysis of the FT-IR spectrum of monosodium urate, as illustrated in Fig. 3, furnishes essential insights into its molecular composition. The varied frequencies unveil noteworthy details pertaining to the bonds and functional groups inherent in the molecule. At 1050 cm^{-1}, vibrations of C-O bonds indicate the potential presence of functional groups, such as ethers. The distinctive peak at 1150 cm^{-1} corresponds to vibrations of C-O-C bonds, a characteristic feature of ethers, thereby contributing to a meticulous characterization of the molecular bonds. The frequency of 1450 cm^{-1} is linked to vibrations of C-H bonds, exposing the existence of carbon-hydrogen bonds within the molecular structure. At 1650 cm^{-1}, a peak signifies vibrations of C=O bonds, typical of carbonyl groups, thus enriching our comprehension of molecular components. Finally, at 1700 cm^{-1}, a distinct peak characteristic of C=O bond vibrations intimates the likely presence of carbonyl groups.

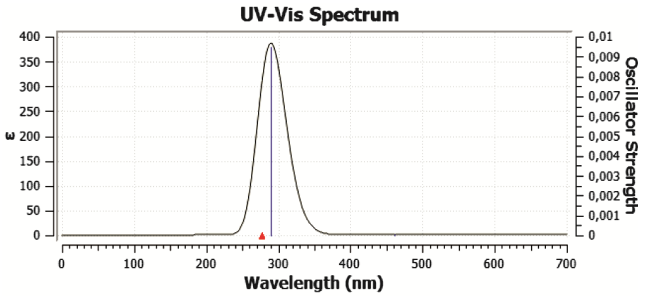

Fig. 2 — UV–Vis spectrum of monosodium urate.

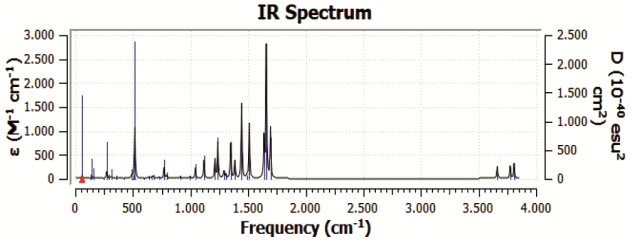

Fig. 3 — FT-IR spectrum of monosodium urate.

In the context of gout, we posit that these electronic and structural properties of monosodium urate potentially play a pivotal role in the pathological processes associated with gout. Notably, vibrations of C-O and C=O bonds, coupled with the presence of carbonyl groups, hint at specific interactions that could influence the crystallization of monosodium urate in the joints a central element in the genesis of gout. These findings make a substantial contribution to the structural delineation of monosodium urate, casting light on its molecular intricacies and their relevance to the pathophysiology of gout.

Theoretical chemical displacements ^{1}H and ^{13}C NMR of the monosodium urate molecule

The analysis of NMR spectroscopy is commonly used to assess the structure of reactive organic compounds by predicting their structural and functional groups. In the case of the specified compound, the ^{13}C and ^{1}H NMR chemical shifts were predicted using the Gauge-Including Atomic Orbital (GIAO)[27-29] approach at the B3LYP theory level, in both gas and water phases. Fig. 4 presents the Raman spectrum of carbon-13 (^{13}C) for the monosodium urate molecule ($NaC_5H_3N_4O_3$), revealing five distinct peaks crucial for characterizing the molecular structure. Each peak, between 185-188 ppm (5-C), 177-181 ppm (3-C), 175-177 ppm (2-C), 171-174 ppm (7-C), and 131-134 ppm (1-C), provides precise details about the specific localization of carbon atoms. The mention of "Degeneracy between 0 and 1" emphasizes a quantum similarity among these peaks, highlighting the significance of molecular symmetry in atomic vibrations.

The carbon-13 Raman spectrum offers a detailed understanding of the molecular structure of monosodium urate, significantly contributing to our knowledge of atomic vibrations and the spatial distribution of carbon atoms in this reactive molecule. These results enrich our understanding of the relationship between the studied molecule and the pathophysiology of gout by providing in-depth insights into its molecular structure and vibrational behavior.

Raman spectroscopy of monosodium urate (MSU) reveals distinct vibrational dynamics of its hydrogen atoms (1H), as shown in Fig. 5. The first peak, centered around 7.15 ppm, corresponds to 15 NH_2 hydrogen atoms and exhibits a degeneracy ranging from 0.2 to 0.65. This relatively low degeneracy suggests restricted rotational freedom due to hydrogen bonding within the NH_2 groups. Conversely, the second peak, at approximately 5.05 ppm, originates from 11H and 13H atoms on the uric acid ring and displays a higher degeneracy between 0.8 and 1.2. This indicates greater vibrational flexibility potentially arising from weaker interactions or more open environments compared to the NH_2 hydrogens. Such contrasting peak characteristics provide valuable insights into the differential dynamics of the two sets of hydrogen atoms within the MSU molecule.

Quantum chemical calculation

Quantum chemical calculations were conducted using Density Functional Theory (DFT) with the 6-311G(d,p) basis set in the Gaussian 09 software package for the monosodium urate Molecule ($NaC_5H_3N_4O_3$). The Natural Bond Orbital (NBO) charge distribution in the B3LYP/6-311G(d,p) model indicates that the most negative charges are localized on specific atoms. This distribution is influenced by the electronegativity of certain constituent atoms. Frontier Molecular Orbitals (FMO), including the Highest Occupied Molecular Orbital (HOMO) and Lowest Unoccupied Molecular Orbital (LUMO), play a pivotal role in elucidating chemical reactivity. The HOMO, without electrons, signifies the electron-donating capacity (E_{HOMO}), while the LUMO, lacking electrons, indicates the electron-accepting capacity (E_{LUMO})[30].

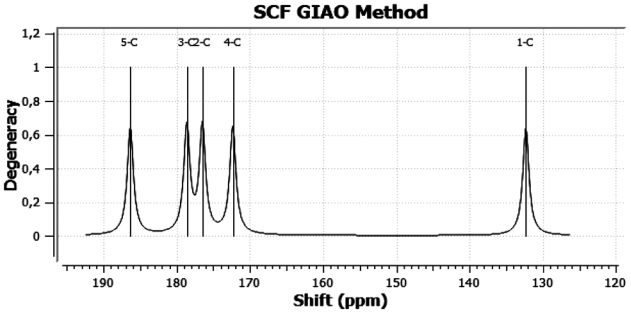

Fig. 4 — Raman spectrum of ^{13}C.

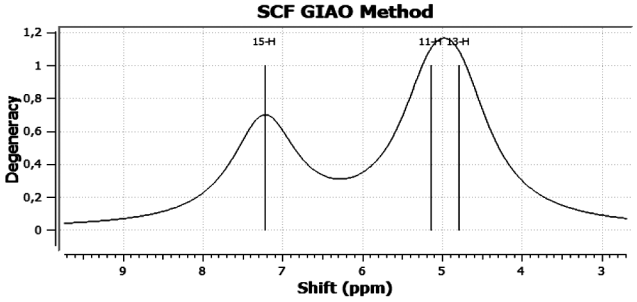

Fig. 5 — Raman spectrum of ^{1}H.

Fig. 6 displays the charge distribution, HOMO, and LUMO calculations for monosodium urate. The HOMO energy (–4.92456 eV) indicates its electron-donating potential, while the LUMO energy (–1.58059 eV) suggests its ability to accept electrons. The large energy gap between them (3.343968 eV) signifies the molecule's resistance to electronic excitations, contributing to its stability. Additionally, the high polarizability (ΔN_{max} = 0.97267) suggests a strong response to electric fields and interactions. These electronic properties influence chemical reactions and stability, potentially impacting gout pathophysiology. Understanding these properties, combined with insights into molecular dynamics, could pave the way for the development of targeted therapies against gout based on the nuanced molecular and electronic characteristics of monosodium urate.

Table 1 presents the local descriptors of monosodium urate obtained from quantum chemical calculations. These descriptors, including atomic charge parameters Hirshfeld and Merz-Kollman, as well as other features such as f^+, f^-, ω^+, and N^- for each atom in the molecule, provide an in-depth view of local electronic properties. The analysis of the data reveals significant variations between atoms, highlighting marked differences in their electronic properties. For instance, sodium atoms (Na14) exhibit high values of f^+ and f^-, indicating a strong positive charge, in accordance with the anticipated ionic nature of sodium. The parameters ω+ and N– unveil nuances in electron distribution, demonstrating notable variability from one atom to another.

This fine characterization of the local electronic properties of monosodium urate offers a profound understanding of how the molecule interacts at the atomic level. These results enrich our knowledge of the underlying mechanisms of monosodium urate, suggesting potential correlations with the pathophysiology of gout. By integrating this data, we broaden our perspective on how these specific electronic properties may influence the formation of monosodium urate crystals, a key process in the development of gout. Thus, these results significantly contribute to our understanding of the effect of

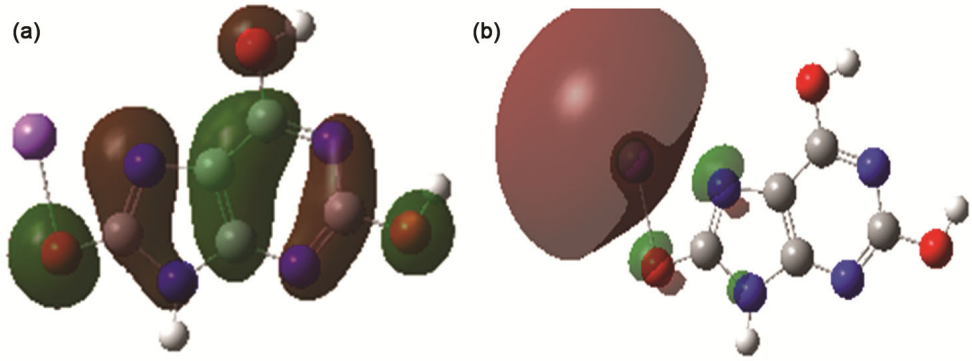

Fig. 6 — (A) HOMO and (B) LUMO of monosodium urate.

Table 1 — Local descriptors of monosodium urate.

	Hirshfeld				Merz-Kollman			
	f^+	f^-	ω^+	N^-	f^+	f^-	ω^+	N^-
C1	0,070686	–0,00297	0,082693896	0,032943669	0,070686	–0,00297	0,245955694	–5,60039254
C2	0,050776	0,007386	0,113144333	–0,013318788	0,050776	0,007386	0,074794183	10,25032491
C3	0,058202	0,015378	0,093822147	0,024713306	0,058202	0,015378	0,055783619	–4,262896486
C4	0,061081	0,005658	0,091656607	0,068078249	0,061081	0,005658	0,045651928	–0,654549319
C5	0,055211	0,001733	0,087675113	0,007559312	0,055211	0,001733	0,112691927	–0,482089459
N6	0,050931	0,01312	0,084353247	0,062789841	0,050931	0,01312	0,092344707	0,96009929
N7	0,05821	0,015279	0,087951935	0,062354325	0,05821	0,015279	0,064977278	1,104868337
N8	0,034989	0,00977	0,174154355	–0,081263715	0,034989	0,00977	0,241659415	–8,468287094
N9	0,111221	–0,01843	0,056024059	0,043484931	0,111221	–0,01843	–0,177893827	3,872629781
O10	0,0787	0,016726	0,225747677	–0,018789401	0,0787	0,016726	0,282964444	–0,919271894
O12	0,062268	–0,00017	0,098480668	–0,001382096	0,062268	–0,00017	0,093523179	0,997806969
O14	0,142116	–0,00424	0,124838883	0,07397549	0,142116	–0,00424	0,156322262	0,355536532
Na14	0,068633	0,911033	0,108126734	4,049706999	0,068633	0,911033	0,061087531	7,119214315

monosodium urate on the presence of gout, paving the way for further investigations and potential applications in the field of medical research.

Table 2 presents the results of an in-depth analysis conducted using second-order perturbation theory of the Fock matrix in the NBO basis for monosodium urate, obtained through the B3LYP/6-31G (d,p) method. These results provide crucial information to understand the impact of the studied molecule on the presence of gout.

Significant interactions between donors and acceptors, such as π-type interactions between C1-C2 (donor) and C3-N7 (acceptor) with substantial interaction energies (E(i,j)) of 0.049, highlight the existence of important electronic bonds. Similar interactions with other atoms and orbitals (C4-N6, C5-N9) underscore the crucial importance of these bonds in the electronic structure of monosodium urate.

σ* interactions with the Lp(1) orbitals of N6, N7, N8, and the Lp(2) orbitals of O10, O12, O14 reveal significant interaction energies, suggesting notable contributions of these orbitals to the electronic stability of the molecule. These results thus provide valuable insights into understanding how the electronic structure of monosodium urate can influence molecular dynamics and, by extension, the pathophysiology of gout. In summary, these findings enrich our understanding of underlying mechanisms and open promising avenues for future investigations into the role of monosodium urate in the context of gout.

The molecular electrostatic potentials (MEP) provide intricate insights for examining the chemical reactivity of a compound. The spatial arrangement and magnitudes of the electrostatic potential play a crucial role in dictating the initiation of a chemical reaction, determining whether it involves the attack of an electrophilic or nucleophilic agent. Moreover, the three-dimensional distribution of the electrostatic potential significantly influences the binding of a substrate to the active site of a receptor[31]. The total electronic density mapped with the electrostatic potential surface, along with the electrostatic contour map of the molecule monosodium urate, is shown in Fig. 7.

The analysis of the Molecular Electrostatic Potential (MESP) of monosodium urate, presented graphically, provides crucial insights into its chemical reactivity, enhancing our understanding of its potential impact on the presence of gout. The color range, reflecting values between –1.439e0 and 1.439e0, highlights various electronic characteristics of the molecule. Red areas, indicating high values,

Table 2 — Monosodium urate: NBO/DFT Analysis.

Donor (i)	Type	ED (i) (e)	Acceptor (j)	Type	ED (j) (e)	E(2)	E(j)-E(i)	E(i,j)
C1 - C2	π	1,96625	C3 - N7	π^*	0,45285	11,54	0,26	0,049
C1 - C2	π	1,96625	C4 - N6	π^*	0,52884	40,85	0,25	0,092
C1 - C2	π	1,96625	C5 - N9	π^*	0,49554	10,65	0,25	0,047
C3 - N7	π	1,75161	C1 - C2	π^*	0,52884	31,51	0,33	0,096
C4 - N6	π	1,76056	C3 - N7	π^*	0,45285	36,47	0,31	0,101
C5 - N9	π	1,87245	C1 - C2	π^*	0,52884	19,03	0,32	0,077
N6	Lp(1)	1,8874	C1 - C4	σ^*	0,04202	9,44	0,91	0,084
N6	Lp(1)	1,8874	C3 - N7	σ^*	0,45285	11,25	0,89	0,091
N7	Lp(1)	1,89619	C1 - C2	σ^*	0,52884	11,04	0,87	0,089
N7	Lp(1)	1,89619	C3 - N6	σ^*	0,04131	11,11	0,87	0,089
N8	Lp(1)	1,65085	C1 - C2	π^*	0,52884	40,62	0,28	0,099
N8	Lp(1)	1,65085	C5 - N9	π^*	0,49554	50,02	0,26	0,105
N9	Lp(1)	1,9016	C5 - N8	σ^*	0,08659	8,75	0,79	0,075
O10	Lp(2)	1,85277	C3 - N7	π^*	0,45285	36,86	0,32	0,105
O12	Lp(2)	1,85277	C4 - N6	π^*	0,52884	36,18	0,32	0,107
O14	Lp(2)	1,86087	C5 - N8	σ^*	0,08659	24,65	0,68	0,117
O14	Lp(2)	1,86087	C5 - N9	σ^*	0,49554	14,42	0,78	0,097
O14	Lp(3)	1,67129	C5 - N9	π^*	0,49554	95,36	0,24	0,141
C3 - N7	π	0,45285	C1 - C2	π^*	0,52884	158,52	0,02	0,075
C4 - N6	π	0,52884	C1 - C2	π^*	0,52884	160,2	0,03	0,086
C5 - N9	π	0,49554	C1 - C2	π^*	0,52884	47,96	0,03	0,045

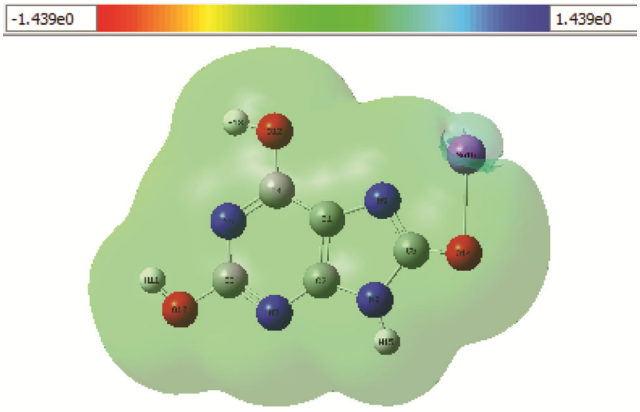

Fig. 7 — Electrostatic potential maps around the molecule monosodium urate.

suggest nucleophilic sites potentially ready to accept electrons in chemical reactions. On the contrary, blue areas, associated with low values, denote an electron deficiency with a propensity to donate electrons. Light blue areas indicate regions slightly deficient in electrons, with a low disposition to provide electrons. Yellow areas, slightly enriched in electrons, may participate in electronic interactions, albeit less pronounced than the red areas. Finally, green areas, neutral, may not play a direct role in chemical reactions involving electron transfers.

This electrostatic analysis provides key information on the reactivity of monosodium urate, suggesting specific areas of the molecule that could actively interact in biochemical processes related to gout. These results strengthen our understanding of how the molecule might influence biological reactions related to gout, opening avenues for further research and potential applications in the development of targeted therapies for this painful condition.

The Density Functional Theory (DFT) study of monosodium urate, conducted using the B3LYP/6-311G(d,p) method, has provided significant insights into its electronic and optical properties (Table 3).

The analysis reveals the potential impact of monosodium urate on the occurrence of gout. The electric dipole moments unveil a specific charge distribution, highlighting the compound's polarization. This feature suggests subtle interactions with external electric fields, which could be relevant in complex biological contexts. The average polarizability indicates the ability of monosodium urate to deform in response to an external electric field, potentially influencing its behavior in specific biological environments, such as joints. Changes in polarizability denote alterations induced by external

Table 3 — DFT dipole moments of monosodium urate (B3LYP/6-311G(d,p)).

	Parameters	DFT
Dipole moment (Debye)	μ_x	6,3679
	μ_y	2,2841
	μ_z	–0,0021
	μ	6,7652
Polarizability (Debye)	α_{xx}	–53,1885
	α_{xy}	19,3923
	α_{yy}	–63,4245
	α_{xz}	–0,0107
	α_{yz}	–0,0079
	α_{zz}	–71,7752
	$< \alpha >$	96,5234
	$\Delta\alpha$	82,0112
First hyperpolarizability (Debye)	β_{xxx}	176,2804
	β_{xxy}	65,3224
	β_{xyy}	0,7590
	β_{yyy}	11,6764
	β_{xxz}	–0,0500
	β_{xyz}	–0,0182
	β_{yyz}	0,0004
	β_{xzz}	–0,0500
	β_{yzz}	5,2850
	β_{zzz}	–0,0135
	β_{tot}	226,9815
Second hyperpolarizability (Debye)	γ_{xxxx}	440,3724
	γ_{yyyy}	–641,2754
	γ_{zzzz}	–67,6722
	γ_{xxyy}	–363,5728
	γ_{yyzz}	–140,8492
	γ_{xxzz}	–337,5703
	γ	898,5086

interactions, emphasizing the sensitivity of monosodium urate to its environment. These changes could be linked to specific biological processes involved in the development of gout. Hyperpolarizabilities provide an in-depth understanding of the nonlinear responses of monosodium urate, indicating significant non-linearity of the material. These properties could influence how the molecule reacts to external stimuli in biological conditions. These results suggest that the distinctive electronic and optical properties of monosodium urate could play a crucial role in biological processes related to gout.

Conclusions

In conclusion, the utilization of advanced density functional theory (DFT) techniques in this study has not only delivered a comprehensive analysis of monosodium urate's conformational stability, molecular structure, vibrational spectra, and electronic properties but has also unearthed new avenues for exploration. The insights gained from this research significantly contribute to our knowledge of the molecular intricacies underlying gout, providing a solid foundation for the development of promising therapeutic interventions. Moreover, the identification of monosodium urate's potential application in environments influenced by electric fields introduces a novel dimension to its significance. The highlighted electronic and optical properties suggest intriguing possibilities for its role beyond gout, opening up opportunities for interdisciplinary studies. This research not only expands our current understanding of gout but also sets the stage for innovative cross-disciplinary collaborations and further investigations into the broader implications of monosodium urate unique characteristics. In essence, the findings presented herein extend beyond the confines of gout pathology, offering a platform for pioneering research initiatives and the potential development of targeted therapies not only within the realm of rheumatic disorders but also in diverse scientific and medical fields. This study serves as a stepping stone towards a more comprehensive comprehension of monosodium urate's multifaceted properties and its potential impact on various biological systems.

References

1 Cramer C J., *Essentials of computational chemistry: theories and models*, (John Wiley & Sons) 2013.

2 Jensen F, *Introduction to computational chemistry*, (John wiley & sons) 2017.

3 Koch W & Holthausen M C, *A chemist's guide to density functional theory*, (John Wiley & Sons) 2015.

4 Neogi T, Jansen T L Th A, Dalbeth N, Fransen J, Schumacher H R, Berendsen D, Brown M, Choi H, Edwards N L, Janssens H J E M, Liote F, Naden R P, Nuki G, Ogdie A, Perez-Ruiz F, Saag K, Singh J A, Sundy J S, Tausche A K, Vaquez-Mellado J, Yarows S A & Taylor W J, *Arth Rheum*, 67 (2015) 2557.

5 De Miguel E, Puig J G, Castillo C, Peiteado D, Torres R J & Martín-Mola E, *Ann Rheu Disea*, (2011) 154997.

6 Chhana A, Callon K E, Dray M, Pool B, Naot D, Gamble G D, Coleman B, McCarthy G, McQueen F M, Cornish J & Dalbeth N, *Ann Rheu Disea*, 73 (2014) 1737.

7 Martillo M A, Nazzal L & Crittenden D B, *Curr Rheum repo*, 16 (2014) 1.

8 Ogdie A, Taylor W J, Neogi T, Fransen J, Jansen T L, Schumacher H R, Louthrenoo W, Vazquez-Mellado J, Eliseev M, McCarthy G, Stamp L K, Perez-Ruiz F, Sivera F, Ea H A, Gerritsen M, Cagnotto G, Cavagna L, Lin C, Chou Y, Tausche A, Ochtrop M L G, Janssen M, Chen G H, Slot O, Lazovskis J, White D, Cimmino M A, Uhlig T & Dalbeth N, *Arth Rheum*, 69 (2017) 429.

9 Pascual E & Sivera F, *Ann Rheu Disea*, 66 (2007) 1269.

10 Khanna D, Fitzgerald J D, Khanna P P, Bae S, Singh M K, Neogi T, Pillinger M H, Merill J, Lee S, Prakash S, Kaldas M, Gogia M, Perez-Ruiz F, Taylor W, Lioté F, Choi H, Singh J A, Dalbeth N, Kaplan S, Niyyar V, Jones D, Yarows S A, Roessler B, Kerr G, King C, Levy G, Furst D E, Edwards N L, Mandell B, Schumacher H R, Robbins M, Wenger N & Terkeltaub R, *Arthr Care Rese*, 64 (2012) 1431.

11 Theophilou A K, *J Chem Phys*, 149 (2018) 074104.

12 Gross A E, Dobson J F & Petersilka M, *Top Curr Chem*, 181 (1996) 81.

13 Neese F, *Coord Chem Rev*, 253 (2009) 526.

14 Midoune A & Messaoudi A, *Comp Rend Chim*, 23 (2020) 143.

15 Becke A D, *J Chem Phys*, 96 (1992) 2155.

16 Neha M, Pooja B, Vimal V, Parvez Ahmad A, Ghanshyam S & Bal Krishna S, *Wor J Cond Matt Phys*, 1 (2011) 70.

17 Hehre W J, Stewart R F & Pople J A, *J Chem Phys*, 51 (1969) 2657.

18 Bonniard L, Kahlal S, Diallo A K, Ornelas C, Roisnel T, Manca G, Rodrigues J, Ruiz J, Astruc D & Saillard J Y, *Inor Chem*, 50 (2011) 114.

19 Geerlings P & De Proft F, *Phys Chem Chem Phys*, 10 (2008) 3028.

20 Ayers P W, Anderson J S & Bartolotti L J, *Inter J Quan Chem*, 101 (2005) 520.

21 Sebastian S, Sylvestre S, Jayabharathi J, Ayyapan S, Amalanathan M, Oudayakumar K & Herman I A, *Spectr Acta Part A: Mol Bio Spec*, 136 (2015) 1107.

22 Szafran M, Komasa A & Bartoszak-Adamska E, *J Mole Struc*, 827 (2007) 101.

23 James C, Raj A A, Reghunathan R, Jayakumar V S & Joe I H, *J Ram Spect*, 37 (2006) 1381.

24 El Ouafy H, Aamor M, Amini L, Oubenali M, Mbarki M, Haimouti A & El Ouafy T, *Curr Chem Lette*, 11 (2022) 291.

25 Othmer K, *Ency Chem Tech*, 14 (2005) 1.

26 Lagutschenkov#A, Langer J, BerdenOomens G & Dopfer J, *Phys Chem Chem Phys*, 13 (2011) 2815.

27 Uludağ N & Serdaroğlu G, *J Mole Struc*, 1155 (2018) 548.

28 Rohlfing C M, Allen L C & Ditchfield R, *Chem Phys*, 87 (1984) 9.

29 Wolinski K, Hinton J F & Pulay P, *J Amer Chem Soc*, 112 (1990) 8251.

30 Bouayad K, Rodi Y K, Elmsellem H, Abdel-Rahman I, El Ghadraoui E H, Chakroune S & Essassi E M, *J Mat Env Sci*, 9 (2018) 474.

31 Gasteiger J, Li X, Rudolph C, Sadowski J & Zupan J, *J Amer Chem Soci*, 116 (1994) 4608.